

Spectromicroscopy of tribological films from engine oil additives. Part I. Films from ZDDP's

G.W. Canning^a, M.L. Suominen Fuller^a, G.M. Bancroft^{a,*}, M. Kasrai^a, J.N. Cutler^b, G. De Stasio^c and B. Gilbert^d

^a Department of Chemistry, University of Western Ontario, London, Ontario, N6A 5B7 Canada
E-mail: gmbancro@uwo.ca

^b Wright Laboratory, Wright-Patterson Air Force Base, OH 45433-7750, USA

^c Istituto di Struttura della Materia, Consiglio Nazionale delle Ricerche, Via Fosso del Cavaliere, I-00133 Rome, Italy

^d Institute de Physique Appliquée, Ecole Polytechnique Fédérale, CH-1015 Lausanne, Switzerland

Received 1 November 1998; accepted 23 February 1999

Antiwear films formed from pure neutral alkyl- and aryl-ZDDP's, and a commercial ZDDP, have been studied with high resolution synchrotron-based photoemission spectromicroscopy with a new instrument, MEPHISTO. Good P L-edge XANES spectra have been taken on areas between 12 and 400 μm^2 , and good images of phosphates and ZDDP have been obtained at $\sim 1 \mu\text{m}$ resolution on both smooth and rough steel. These spectra, and corresponding images, show immediately that both the chemistry and the morphology of the alkyl and aryl films are very different. The alkyl film contains a range of smaller and larger protective polyphosphate pads from a few to $\sim 25 \mu\text{m}^2$ in area. We have shown that the chemistry of small and large pads are different. The large pads contain very long chain polyphosphate; while the smaller pads contain short chain polyphosphate. The aryl films contain ortho- or pyro-phosphates, are much thinner and more uniform, with obviously more streaking from initial wear, and no obvious protective pad formation. Antiwear films generated from the commercial ZDDP, rubbed in base oil, show that the long chain polyphosphate is converted to ortho- or pyro-phosphate, but the amount and distribution of phosphate does not change noticeably. The antiwear films are remarkably stable physically.

Keywords: XANES, microscopy, X-ray absorption, antiwear film

1. Introduction

Zinc dialkyl (or diaryl) dithiophosphates (ZDDP's) have been the most prominent antiwear additives in lubricating oils for over forty years [1]. ZDDP's act as antiwear agents by forming a very thin protective film at the rubbing surfaces [2].

Much information regarding the chemistry of the films, and the mechanism of formation, has been published. For example, Sheasby et al. [3] using electron probe micro analysis (EPMA) in conjunction with secondary electron microscopy–energy dispersive X-ray analysis (SEM–EDX) showed that the film contained Zn, S, P, C and O. Using X-ray fluorescence (XRF), Rounds [4] found mainly Zn, S and P. Newer techniques such as X-ray photoelectron spectroscopy (XPS), Auger electron spectroscopy (AES), reflectance-absorbance infrared spectroscopy and X-ray absorption spectroscopy (XAS) have been used to provide the chemical differentiation for different elements. For example, Bird and Galvin [5], using XPS, found that the film consisted of Zn, P, S, O and Fe, and that the P was present as a phosphate and the S as a sulfide. Spedding and Watkins [6], using XPS, agreed with this conclusion and found that Zn was mainly associated with phosphate. Jahanmir [7], using the Auger microprobe, showed that the film is several hundred Å thick and is composed of iron

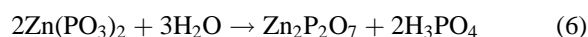
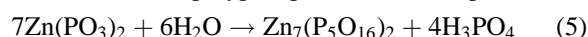
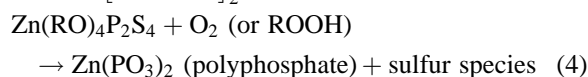
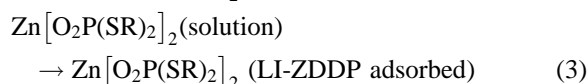
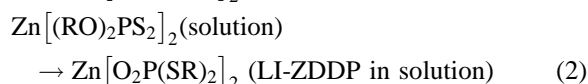
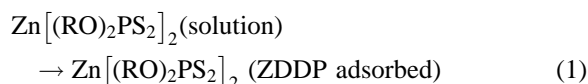
sulfide and zinc phosphate. Willermet et al. [8,9] using reflectance infrared spectroscopy, XPS, and Auger, found that the films were inorganic, amorphous phosphate films (mostly ortho- and pyro-phosphate) with the cation derived from the lubricant additives. Willermet et al. [9,10] used AES depth profiling, surface profilometry, and SEM/EPMA to obtain an average thickness of a ZDDP film of 530 Å. Bell et al. [11,12] applied time of flight–secondary ion mass spectroscopy (TOF–SIMS) and XPS to confirm that their antiwear film was polyphosphate.

X-ray absorption techniques have recently been useful for obtaining the mechanism of decomposition. The P and S L-edge XANES was used by Yin et al. [13–15] and Fuller et al. [16,17] to chemically speciate the films using TEY and FY methods. These give analysis depths of about 50 and 500 Å, respectively [18], ideal for the analysis of these thin films. The antiwear films showed a layered structure, with the surface consisting of adsorbed ZDDP and long chain polyphosphate, and the bulk composed of iron oxide intergrown with a short chain polyphosphate. A mechanism consistent with these observations was then proposed [14, 19].

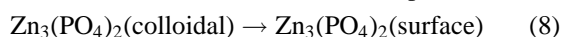
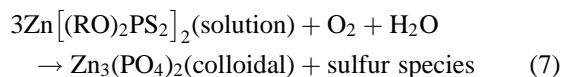
In her studies of heated oils, Suominen Fuller et al. [17] found evidence for a linkage isomer of ZDDP with O bonded to Zn instead of S. Also, from P K-edge spectra, there was no evidence for iron phosphates. The mechanism

* To whom correspondence should be addressed.

was then modified to:



Suominen Fuller et al. [17] also obtained evidence for film formation from solution decomposition and proposed the following:



Very recently, Martin and his collaborators [20,21] have used energy-filtering transmission electron microscopy (EFTEM) coupled with electron energy loss spectroscopy (EELS) and EDX to image and analyse the wear debris of tribofilms.

The chemistry of these films is now quite well established, but nearly all of the above studies have analysed several mm^2 of the antiwear films, and thus an ‘‘average’’ chemical composition has been obtained. Only a few studies have analysed the spatial nature of these films or the chemistry at the micron level. Jahanmir [7] and Cao et al. [22] using Auger spectroscopy, and Bell et al. [11] using SIMS, did note that the films are very inhomogeneous and ‘‘patchy’’ from their analysis. These studies and many others used the ‘‘traditional’’ SEM imaging technique to show the spatial inhomogeneity of the films at the $10 \mu\text{m}$ level. However, SEM is not well suited to characterize the film morphology, because the SEM analysis depth is $\geq 1000 \text{ \AA}$, and there is no elemental sensitivity for the light elements. In principle, scanning Auger microscopy (SAM) could be very useful for obtaining elemental images of these films; sub-micron resolution is easily obtained, and the analysis depth of $50\text{--}100 \text{ \AA}$ is well suited. Several SAM papers [23,24] have shown only backscattered or secondary electron images of wear tracks. There appear to be no elemental Auger images of these wear films in the literature.

Very recently, XPS using synchrotron radiation has been used to probe $100 \times 30 \mu\text{m}^2$ areas of antiwear films [25]. Using variable photon energy, the chemical sensitivity can be enhanced. Again, the lateral and chemical inhomogeneity of the antiwear films was confirmed, but no chemical information was obtained. Atomic force microscopy (AFM) has also been utilized to show the patchy nature of the

films [26–28], with larger smooth areas (tens of μm^2) and mottled troughs (a few μm^2). The latter showed, with interfacial force microscopy (IFM), that the large patches are very hard and elastic. The AFM and IFM will be extremely useful for studies of these films, but of course, no chemical information is easily attainable.

X-ray spectromicroscopy has been developed recently, mainly at synchrotron sources, to access the high flux and tunable energy of synchrotron radiation. For surface studies, scanning photoelectron and photoemission microscopes (SPEM) have enormous potential [29]. The first paper in the antiwear field was published recently. The elemental images on steel surfaces show the inhomogeneity of the films, and the potential problems of surface roughness. The electron resolution of $\sim 4 \text{ eV}$ precluded any chemical analysis of the elements [30].

The photoemission microscope (so-called PEEM) of Tonner et al. [31] would appear to be ideal for studying the spatial distribution of most chemical species on antiwear films at the micron level. These microscopes image secondary electrons, using conventional SEM optics, emitted after resonance excitation of a core electron to an antibonding level. The escape depth for these secondary electrons is between 50 and 100 \AA , providing maximum contrast for films about a 100 \AA or thicker. The energy resolution (determined partly by the monochromator for P 2p and S 2p spectra) is normally about 0.2 eV , giving the chemical sensitivity of a XANES experiment.

The latest version of this technique – called MEPHISTO (microscope à emission de photoelectrons par illumination synchrotronique de type onduleur – photoelectron emission microscope by synchrotron undulator illumination) has been recently commissioned [32]. This instrument allows secondary electron microimages to be obtained, as well as high resolution X-ray absorption spectra from selected areas within these images. In this paper, we explore the use of this technique for the first time, in detailed chemical and morphological studies of antiwear films. The objectives are the following:

- (1) To confirm whether the micro analysis of these films is similar to the previous macro analyses. Does the chemistry differ in different areas?
- (2) To obtain the difference in morphology and chemistry of films from two different ZDDP’s with different antiwear capabilities.
- (3) To investigate the possibilities of imaging different chemical states of P on steel substrates.

2. Experimental

2.1. Materials and film preparation

The additives used in this study were commercial products and were used without further purification. The blended neutral alkyl and aryl ZDDP oil solutions were

obtained from Chevron, Richmond, CA [16]. The alkyl (di-isopropyl) and aryl (di-*p*-TOP) ZDDP's, both in the neutral form, were used to produce the tribochemical films on the "smooth" 52100 steel. The "smooth" steel AW films were prepared using 52100 steel polished first with 0.25 μm diamond paste, and then with 500 Å alumina paste. The commercial ZDDP was obtained in a pre-concentrated form from Imperial Oil, Sarnia. The commercial ZDDP concentrate was diluted using MCT-10 oil to give the desired concentration by weight. MCT-10 base oil is a mineral oil with a maximum S content of 0.25 mass per cent. The commercial ZDDP, a mixture of the neutral and basic forms, consisting of secondary butyl (85%) and *n*-octyl (15%) groups, was used to produce the tribochemical and thermal films on the "rough" A2 steel. The A2 steel coupons and pins were polished with 320 grit then 600 grit alumina paper. The coupons and cylindrical pins were cleaned in an ultrasonic bath using light hydrocarbon solvent prior to sample preparation. The coupons and 52100 steel pins were both ultrasonically cleaned in light hydrocarbons. Profilometry showed that the A2 steel coupons had an average Ra of 1000 Å, whereas AFM (atomic force microscopy) was used to determine that the highly polished 52100 coupons had an average Ra of less than 50 Å.

Thermally deposited films were made in an oil solution containing the desired concentration of the commercial ZDDP [17]. The steel coupon was suspended in the oil solution and the solution was heated in a temperature controlled bath at 150 °C for 6 h. After the process, the excess oil was gently removed from the surface by dabbing with a paper towel.

The antiwear films were generated on A2 or 52100 steel coupons in a Plint reciprocating wear rig at 100 °C and 25 Hz, with an applied load of 220 N. The cylindrical pin (11.05 mm in length with a radius of 3.11 mm), identical in composition to the metal coupon being used, was loaded against the coupon in the oil containing the additive and was rubbed for the desired length of time. After the test, the excess oil was gently blotted from the surface with a tissue paper.

The "rubbed" antiwear films were prepared by first using the antiwear film preparation to create a film on a coupon. The additive-containing oil was then removed from the rig and replaced with MCT-10 oil without removing the steel coupon or the pin so as to ensure that the pin-coupon contact position remained intact. The sample was then rubbed in the base oil for the desired length of time. Upon removing the coupon from the rig the excess oil was blotted from the surface.

In the case of the "rubbed" thermal film, a thermal film was created as per the above preparation. This coupon was loaded into the Plint rig and rubbed for the desired length of time in MCT-10 base oil with no additive present. Again, after the coupon was removed from the rig the excess oil was gently blotted from the surface with a tissue [13,14,19, 33].

2.2. X-ray absorption and MEPHISTO analysis

Photoabsorption spectra of the samples (analysis area $\sim 5 \text{ mm}^2$) were collected at the Canadian Synchrotron Radiation Facility (CSRF) – Madison, Wisconsin [34]. For P and S L-edge measurements, the Grasshopper soft X-ray beamline, monochromatized by an 1800 grooves/mm grating, was employed. The photon resolution was $< 0.2 \text{ eV}$. The total electron yield (TEY) was measured by directly monitoring the sample current as described previously [35]. The energy scale at the Grasshopper beamline was calibrated with reference to the lowest pre-edge peak of elemental sulfur at 162.7 eV.

The analysis of the films produced was also performed at the Synchrotron Radiation Center – University of Wisconsin using the MEPHISTO system connected to the 6-meter TGM (toroidal grating monochromator) beamline. The samples were rinsed with a light hydrocarbon solvent prior to entry into the vacuum chamber to remove any excess oil. Previous studies illustrated that this did not affect the films' chemical nature [13,14,33].

The MEPHISTO analysis [32] consisted of acquiring microscopic images of photoelectron intensity from various areas on the sample. These show the emitted electron intensity over the observed sample area and are obtained by capturing an image of the emitted electrons on a phosphor screen at a specific photon energy. The electron intensity images can provide detailed chemical maps showing the spatial distribution of a given element or even a given element in a specific chemical environment. This is accomplished by taking microimages at photon energies above and below the edge of the relevant element. The subtraction of the image taken below the edge from that taken above the edge yields a "difference" image. This "difference" image reveals the spatial distribution of the given element in the specific chemical environment.

X-ray absorption spectra of selected areas inside the images were also obtained. Unlike the conventional X-ray absorption technique, where the area being sampled is 5 mm^2 and the spectrum is an average of the entire surface of the sample, MEPHISTO allows for spectra to be obtained from a few hundred μm^2 quickly, or a few tens of μm^2 after multi-scanning. The spectra are obtained by taking the electron emission intensity near the P and S L-edge and the Fe M-edge as a function of photon energy. The spectra provide precise chemical information of areas within the sample including elemental composition and oxidation state [32].

The MEPHISTO analysis of the ZDDP films consisted of obtaining X-ray absorption spectra and images of the samples as outlined above. The pixel size of the image was $\sim 720 \times 568$ and each image took $\sim 10 \text{ s}$ to record. The spectra presented have been normalized for I_0 . The difference images presented were created through digital subtraction of an image captured at the peak energy of the species of interest and an image obtained below the peak. This procedure removes contrast created by surface

roughness. The X-ray absorption near-edge (XANES) spectroscopy spectra presented have all been normalized and represent an average of at least three scans.

3. Results and discussion

3.1. Alkyl and aryl ZDDP – smooth steel ($R_a < 50 \text{ \AA}$)

Alkyl and aryl ZDDP's were tested on extremely smooth steel to investigate if there were spatial physical and chemical differences between the two additives. The hope was that any differences found might explain why the two additives have different wear protection ability. The films analysed were rubbed in the ZDDP oil solution for 60 min. The spectra were obtained from $400 \mu\text{m}^2$ areas inside and outside rubbing areas.

The spectrum shown in figure 1(a) (top) shows a classic polyphosphate spectrum, very similar to those obtained by Yin et al. [13,14] and Fuller et al. [16]. The shoulders at 135.5 and 136.5 eV (a and b in figure 1(a)) are very intense, characteristic of a long chain polyphosphate. There is no noticeable contamination from undecomposed ZDDP at 135 eV on this very smooth steel. The intensity of the peak outside the rubbed region (figure 1(a), bottom) is very weak showing very little polyphosphate. Figure 1(a) (top) shows that a spectrum of similar quality can be obtained on a $400 \mu\text{m}^2$ area compared to the 5 mm^2 areas obtained previously [13,14,16,17].

The difference images shown in figures 1(b), (c) and (d) were taken at 138 eV with a background image at 133 eV subtracted. The bright areas on the difference images are where phosphate is present. Figure 1(b) shows that the phosphate is concentrated in the area where rubbing occurred. The phosphate has a very patchy appearance. In looking at other areas within the film (figures 1(c) and (d)), this patchy appearance is consistent throughout. There is little directional character to the film in figure 1(b), but more directional character in figure 1(c). The high resolution image in figure 1(d) shows large pads (up to $10 \mu\text{m}$ in diameter) and much smaller pads.

This film is characteristic of a “good” antiwear film, and relatively little wear occurs [14,17]. The larger phosphate pads withstand the pressure applied by the pin. In figure 1(d) some “masking” is evident, especially on the right hand side of the largest bright pads at the bottom. This dark “ring” around the bright spot is generated by the MEPHISTO analysis. The photon beam hits the surface at 30° to the sample. MEPHISTO uses an aperture to prevent stray electrons from influencing the images obtained. This aperture prevents electrons which are not emitted perpendicular ($\pm 3^\circ$) to the surface from being captured. Since the surface on which this film was formed was very smooth and no visible wear direction is observed, any topography shown is caused by the film formed and not the substrate.

Figure 1(a) shows that the chemistry of $\sim 400 \mu\text{m}^2$ of the film is very similar to the chemistry over 5 mm^2 . But, is the

chemistry of the large pads (figure 1(d) bottom) different than the chemistry of the small pads?

The spectra in figure 2 (taken with many scans) although noisy, show that indeed, the chain length of the phosphate is very different for different areas on the surface. Curve A shows a short chain polyphosphate spectrum (peaks a and b are relatively weak) taken from a $70 \mu\text{m}^2$ area where there is only small pad formation (figure 1(d), top). Curves B and C were taken from two large pads (figure 1(d), bottom) (analysis areas 12 and $20 \mu\text{m}^2$, respectively) which show well resolved long chain polyphosphate spectra (peaks a and b are intense). These spectra show that the large load-carrying pads are long chain polyphosphates – at least on the surface. We showed earlier that the bulk of all of these films are ortho and/or pyrophosphates [13,14,16].

Graham et al. [28] have recently shown that the mechanical properties of the large pads vary greatly *across* the large pads with the centre of the pad being very hard and elastic, and the sides of the pads being less hard and less elastic. This difference in mechanical properties probably reflects different chemistries across the large pads. To see this expected difference, we need to obtain spectra over a few μm^2 of the large pads and we have not been successful so far in getting good enough spectra to prove the difference in chemistry. However, with the evidence from the large and smaller pads (figure 2) we suggest that the longest chain polyphosphate will be present at the top of the pad (where the load is the highest), and the phosphate chain length decreases to the edge of the large pads – probably similar to that shown in curve A for the small pads.

The aryl ZDDP spectra and the morphology of the film (figure 3) are quite different than for the alkyl ZDDP. Again, phosphate builds up only in the rubbed region, but the amount of phosphate is much smaller than in figure 2 as indicated by the noise in the spectrum (figure 3(a)). This phosphate spectrum is close to an orthophosphate spectrum because of the weak peaks at 135.5 and 136.5 eV. The aryl film has a very different appearance to that of the alkyl film. In looking at figure 3(b), the film looks very streaky, with no signs of pad formation. The rubbed region is very rough with many gouges in the wear direction (left to right). Figure 3(c) is a difference image obtained at the bottom of the rubbed region. The film appears to have a relatively uniform streaky appearance here as well with the rubbing direction up and down. It has been reported that the aryl ZDDP does not break down as quickly as the alkyl ZDDP [36,37], and wear is higher with aryl ZDDP's than with alkyl ZDDP's. Indeed, the wear scar width on the pin for the aryl film of $\sim 30 \mu\text{m}$ is somewhat larger than the $\sim 20 \mu\text{m}$ wear scar width for the pin in the alkyl film. The alkyl ZDDP formed a phosphate film quickly, thus preventing substantial wear to the coupon, whereas the aryl ZDDP left the coupon exposed to this wear prior to film formation. The coupon was scarred by the wear particles created by the rubbing of the two metal surfaces and these created the striations in the coupon. By the time the aryl ZDDP formed a protective film damage had already occurred.

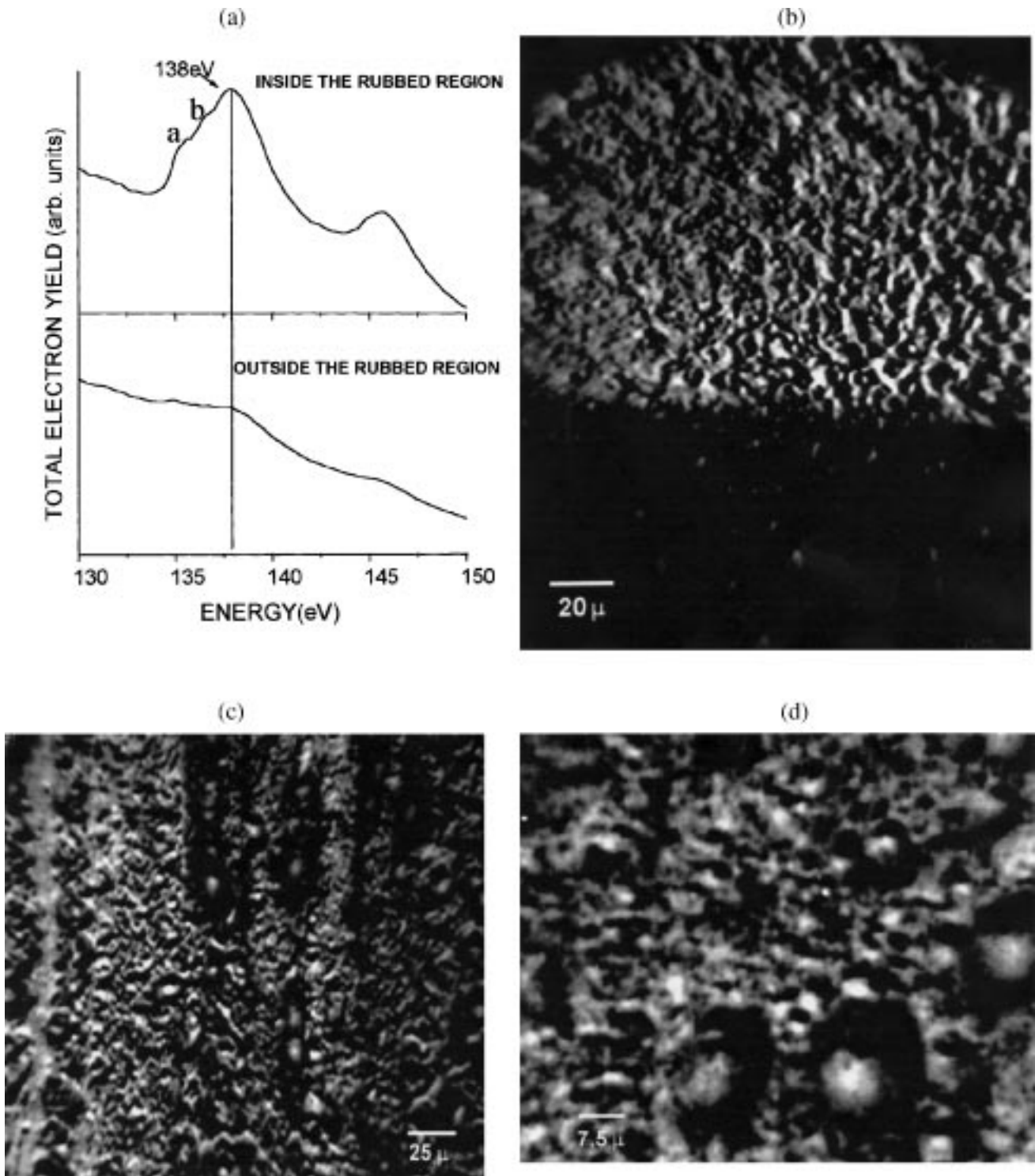


Figure 1. MEPHISTO P L-edge spectra and images of an alkyl ZDDP tribochemical film on very smooth steel: (a) P spectra; (b), (c), (d) are secondary electron images (138 eV minus 133 eV), with (b) taken at the edge of the rubbed area, (c) taken in the rubbed area, and (d) a higher resolution image in the rubbed area.

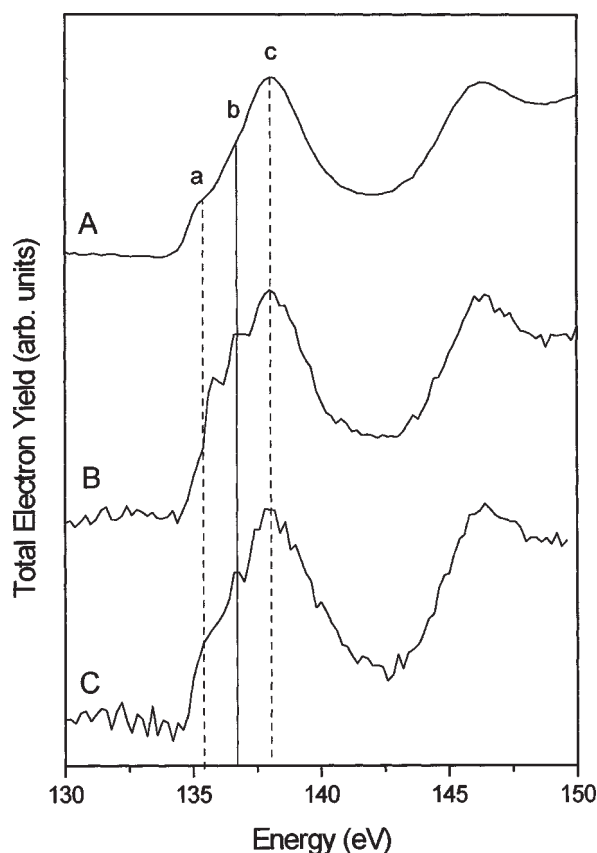


Figure 2. MEPHISTO P L-edge spectra from very small spots on the sample from figure 1. Spectrum A is from a $70 \mu\text{m}^2$ area in the small pad area (top figure 1(d)); spectra B and C are from 12 and $20 \mu\text{m}^2$ areas covering the large pads (bottom, figure 1(d)).

3.2. Rubbed ZDDP thermal film – rough steel

Can we obtain good images off much rougher steels? The previous SPEM imaging study [30] indicated large topographical features. To show that meaningful images of phosphate films on rough steel could be obtained, we first took spectra and images of a rubbed “thermal” film. The thermal film [17] was produced by a 1% commercial ZDDP solution at 150°C , yielding a thin ($\sim 100 \text{ \AA}$) phosphate film caused by the ZDDP decomposition on the hot steel surface. This film was then rubbed in base oil (with no ZDDP) for 30 min. Figure 4 illustrates spectra from $\sim 100 \mu\text{m}^2$ of the rubbed and unrubbed region of the sample (area 1 is the rubbed region, and area 2 is the unrubbed region). The peak at 57.7 eV , which corresponds to the Fe 3p absorption, is more intense in the spectrum taken from inside the rubbed region (area 1) than outside the rubbed region (area 2). The relative intensity of the P 2p signal at 138 eV is opposite to the Fe 3p signal: the P intensity is greater outside the rubbed region (area 2) than inside (area 1). Figure 4(b) is a difference image taken at 57.7 eV , which shows that the iron distribution (blue area) is concentrated in the rubbed region; while the difference image in figure 4(c) was taken at 138 eV showing that the phosphate (red area) is concentrated outside the rubbed re-

gion with some phosphate lying in scratches in the rubbed region.

Overlapping the difference images (figure 4(d)) shows that the iron and the phosphate clearly inhabit the opposite areas. This illustrates that the thermal phosphate coating was not durable enough to withstand the rubbing, and was worn away, exposing the iron substrate below. This rubbing action removed the phosphate on the “peaks” of the surface exposing the iron, but the “valleys” are still covered with phosphate along with the unworn metal. It has been noted before that these thermal coatings are not durable [39], so they are removed during the rubbing. Previous XANES spectroscopy showed that the phosphate remained on the surface after rubbing, but the large analysis area made it impossible to tell whether the phosphate was inside or outside the wear region.

These difference images show that topological effects, although present, are certainly not dominating these difference images on rough steel. The vast majority of the difference image in figure 4(d) is dominated by red (phosphate) or blue (iron). Some of the remaining white areas are due to inhomogeneity of the films with some (a few percent of the total difference image) due to instrumental and topological effects.

3.3. ZDDP antiwear film – rough steel

The film analysed was produced with a 1% commercial ZDDP solution which was rubbed for 30 min. Figure 5(ai) is the spectrum obtained of this sample using the conventional XANES analysis on a 5 mm^2 area. Previous studies [13,14,19,33] show that the signal at 138 and 136.5 eV is from the ZDDP’s conversion to polyphosphate with a signal at 135 eV due to largely unreacted ZDDP. Spectra were obtained using MEPHISTO from $400 \mu\text{m}^2$ areas inside the wear track (area 1 on figure 5(b)) and outside of this region (area 2 on figure 5(b)). Figure 5(aii) is the spectrum obtained from inside the rubbed region and figure 5(aiii) is obtained outside the rubbed region. The spectrum from MEPHISTO (figure 5(aii)) is qualitatively similar to the conventional XANES spectrum [13,14,19,33]. The phosphate signal at 138 eV is greater inside than outside the rubbed region. There is a signal at 135 eV which is attributed to undecomposed ZDDP, and is relatively more intense for the unworn substrate. This peak was not present on our spectrum (figure 1(a)) from smooth steel. These differences are expected from previous work [13,14,19,33] where the ZDDP is converted to a phosphate in wear situations. Undecomposed ZDDP in figure 5(b) is trapped in “valleys” of the rough steel.

Figure 5(b) illustrates the phosphate coverage on the sample (image taken at 138 eV with subtraction of background at 133 eV). The phosphate coverage (red area) is prevalent in the region where the rubbing was taking place (figure 5(b), top). In looking at the intensity map of the ZDDP (figure 5(c)) (image taken at 135 eV with subtraction of background at 133 eV), ZDDP is present over all

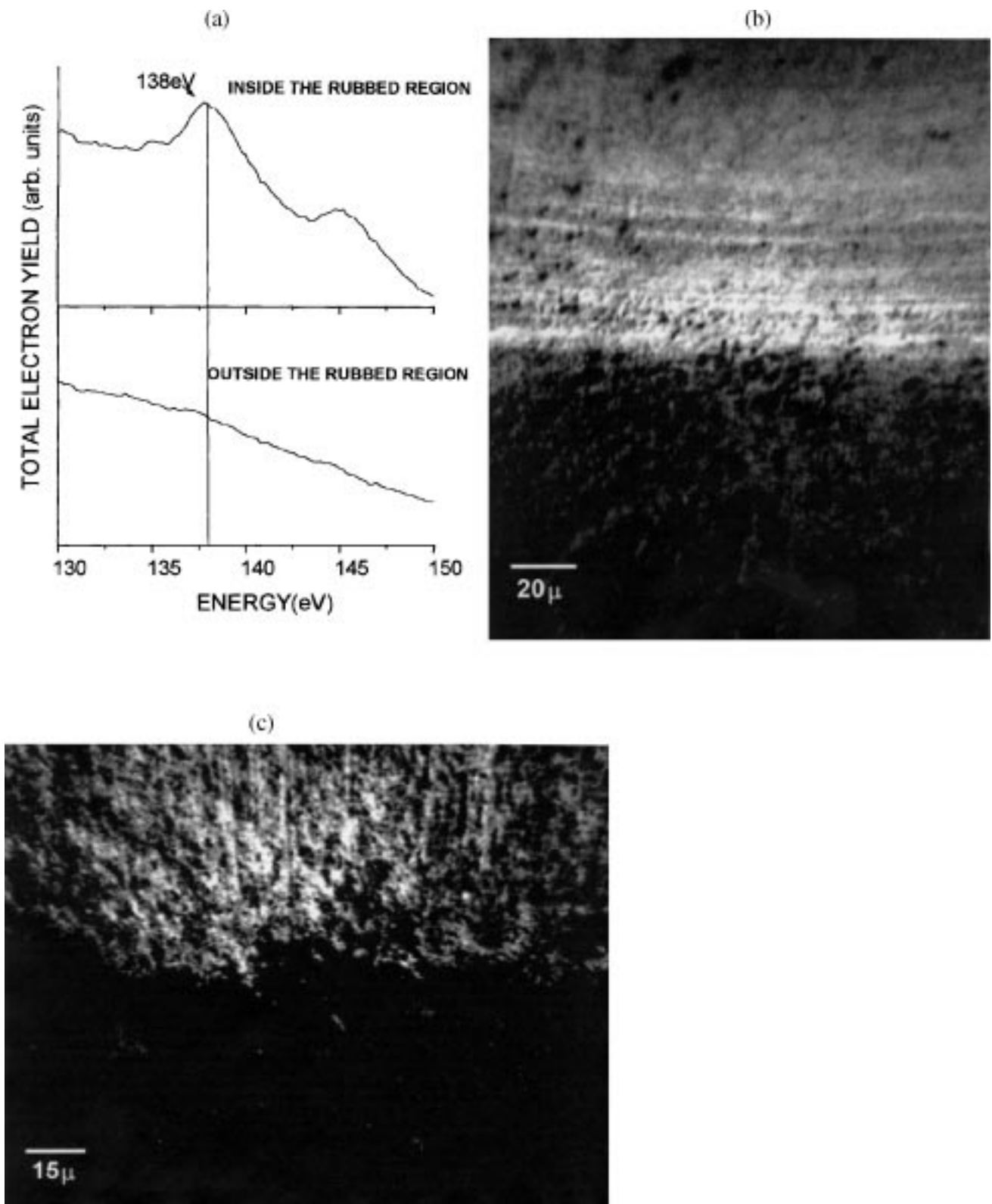


Figure 3. MEPHISTO P L-edge spectra and images of aryl ZDDP tribochemical film on smooth steel: (a) P L-edge spectra; (b) and (c) images at the edges of the rubbed area, where the rubbing direction is across the page in (b), and up and down in (c).

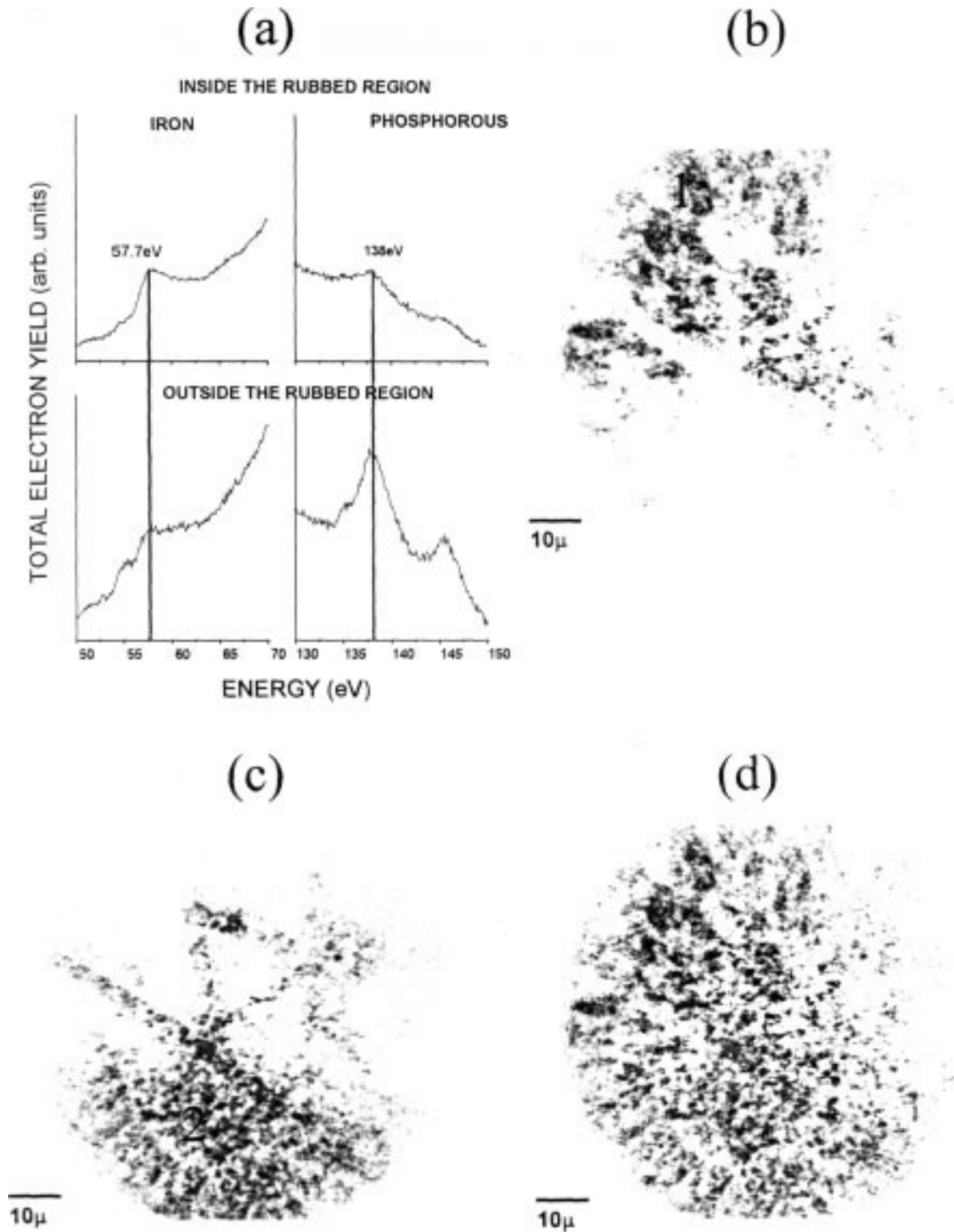


Figure 4. MEPHISTO Fe M-edge and P L-edge spectra and images of ZDDP thermal film rubbed for 30 min ((a) spectra; (b) iron distribution; (c) phosphate distribution; (d) overlapped images). Region 1 is the rubbed area; region 2 is the unrubbed area.

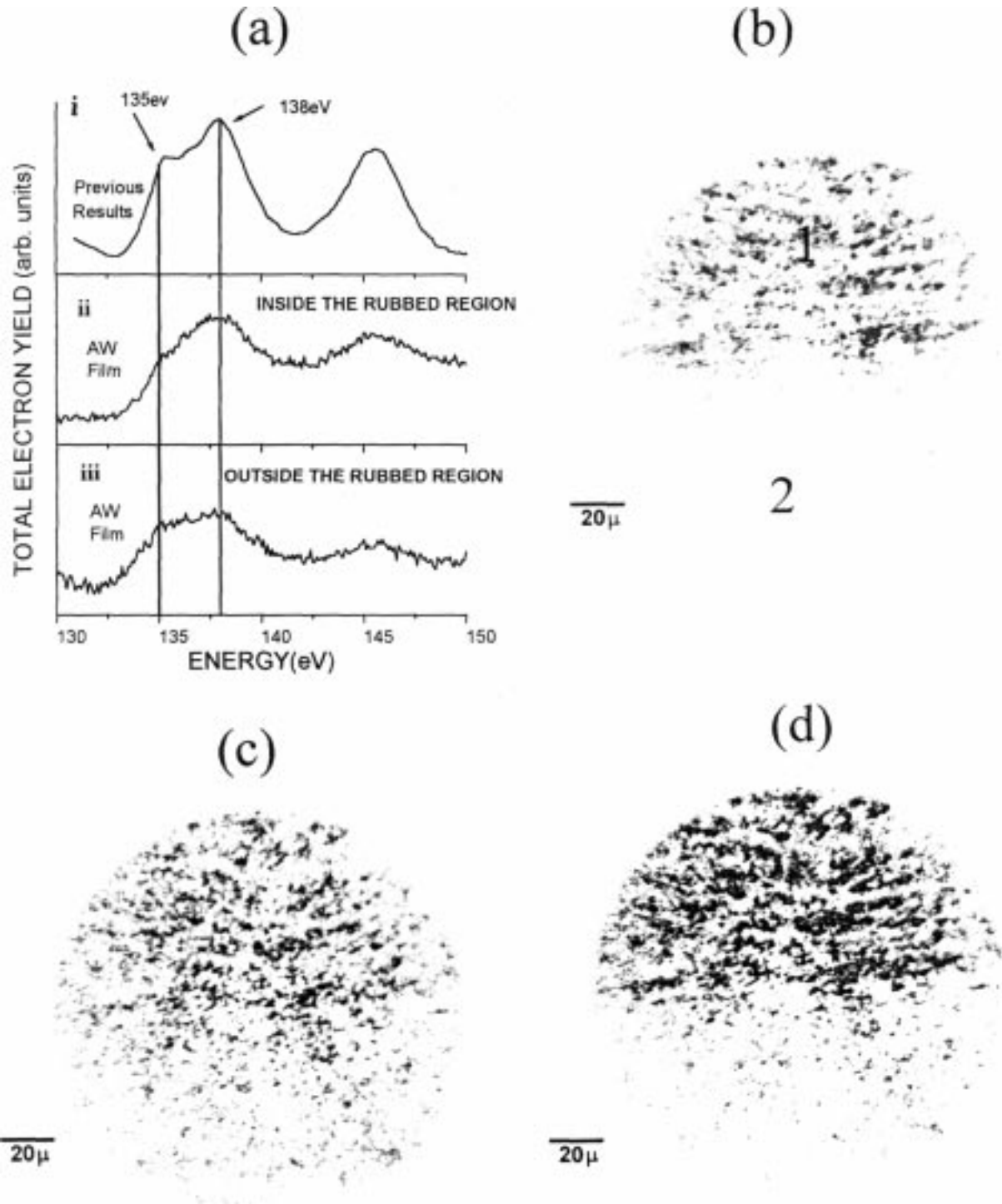


Figure 5. MEPHISTO P L-edge spectra and images of ZDDP-1 tribochemical film on rough steel ((a) spectra; (b) phosphate distribution; (c) unreacted ZDDP distribution; (d) overlapped image).

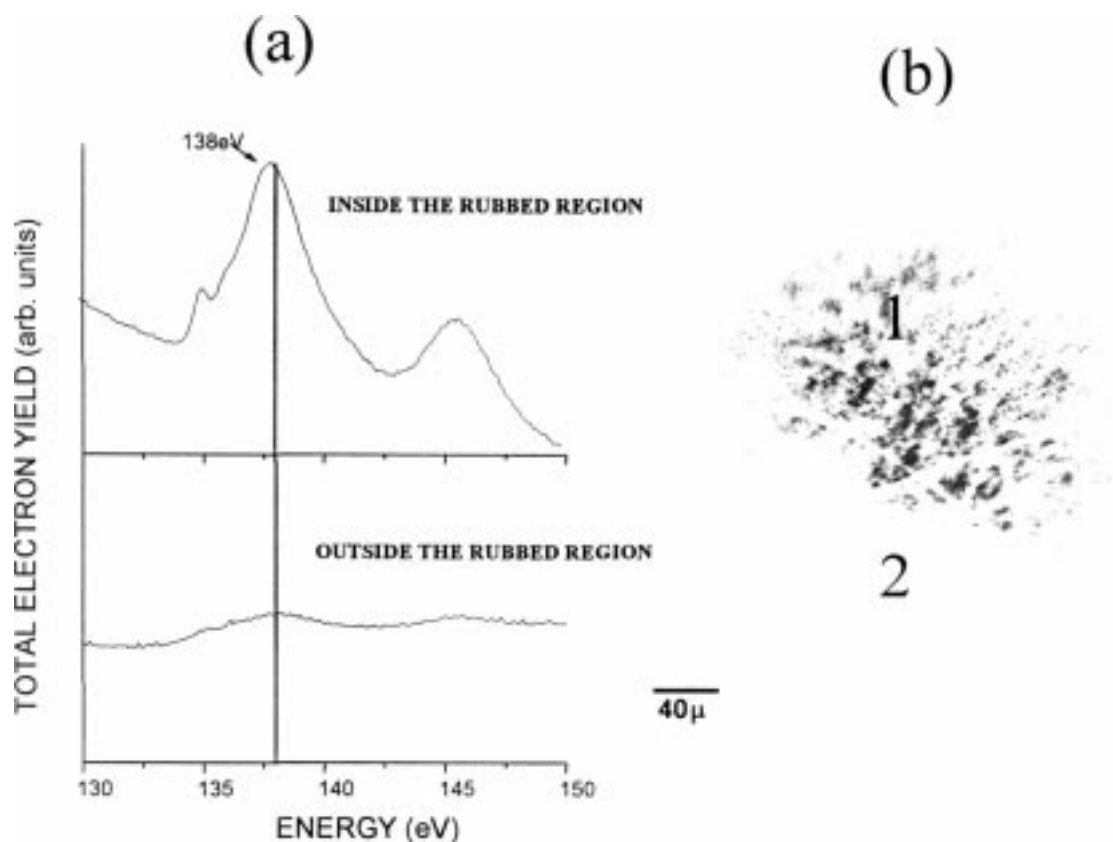


Figure 6. MEPHISTO P L-edge spectra and images of rubbed ZDDP-1 tribochemical film on rough steel ((a) spectra; (b) phosphate distribution).

of the substrate and is represented by the blue areas. Figure 5(d) is a composite difference image created by overlapping those in figures 5(b) and (c). The colours for phosphate and ZDDP remain the same, with any areas where both colours are present (overlap) showing up as green. In the rubbed area (area 1), the undecomposed species is prominent in areas lacking in phosphate. In the areas where the asperities of the coupon break through the oil film, the phosphate film is formed to protect the surface. Since the coupon is rough, this is likely to occur in many areas. The increased temperature and pressure induced at these areas or “peaks” will induce film formation, while areas which are not subject to these conditions or “valleys” only have adsorbed ZDDP. This correlates with IFM data obtained by Warren et al. [27] which found two distinct materials on the surface of a ZDDP AW film. The green areas present are most likely due to overlap in the phosphate and ZDDP peak signals.

3.4. Rubbed ZDDP antiwear film – rough steel

The analysed film was produced with a 1% commercial ZDDP solution which was rubbed for 30 min and then rubbed in base oil for 24 h. The excellent spectrum shows low intensity at 135.3 and 136.5 eV and is characteristic of a short chain polyphosphate. The conversion of long chain to short chain by rubbing without ZDDP has been noted by Yin [19] previously and by Suominen Fuller et al. [17].

This film is very similar in appearance to previous antiwear film (figure 5). Figure 6(b) illustrates the phosphate coverage on the sample. The phosphate (in red) is found solely in the wear track. The additional rubbing has not affected the phosphate film appreciably and illustrates the durability of the film. This reinforces the idea that once the film is formed it is not removed and replaced by a new film upon rubbing, but remains on the surface [39]. Indeed, Suominen Fuller et al. [40] have shown little or no change in film thickness after rubbing an antiwear film in base oil for up to 24 h.

4. Conclusions

Photoemission microscopy using MEPHISTO has been used for the first time to examine the chemistry and morphology of antiwear films at the micron level.

The results show that this technique is extremely useful for obtaining the micro-chemistry and morphology of the films, and confirm that:

- (1) Excellent XANES spectra can be obtained on $400 \mu\text{m}^2$ areas compared to the 5mm^2 areas previously obtained by analysis. Good spectra from areas as small as $12 \mu\text{m}^2$ have also been obtained.
- (2) The microchemistry of the films from neutral alkyl and aryl ZDDP's are quite different, with long chain and short chain polyphosphate forming, respectively. The

long chain polyphosphate from the commercial (alkyl) ZDDP converts to short chain polyphosphate upon further rubbing in base oil, confirming previous observations at the macro level.

- (3) XANES spectra taken on large pads and a number of smaller pads of the alkyl ZDDP film shows that the chemistry is different: the large pads are composed of longer chain length polyphosphates compared to the smaller pads.
- (4) The Fe and P difference images on the rubbed thermal film show that the images are not greatly affected by the surface topography on rough steel.
- (5) The morphology of the alkyl and the aryl films are very different. The alkyl ZDDP decomposed rapidly to give protective pads of about 1–10 μm in diameter. In contrast, the much lower decomposition rate of the aryl ZDDP yields much slower, more uniform, formation of phosphate after a lot of wear has already occurred. There is no evidence of protective pad formation.
- (6) Different P chemical species (ZDDP and phosphate) can be readily imaged, and it appears that most of the ZDDP does not overlap spatially with the phosphate film. Phosphate is formed on the asperities, while adsorbed ZDDP remains in the valleys.

Acknowledgement

This study was financially supported by the National Science and Research Engineering Council (NSERC) and the National Research Council (NRC). We are grateful to P.A. Baudat and J. Retondo for instrument assistance, along with Dr. K. Tan for his assistance with “normal” XANES spectra. We are also grateful to Dr. J. Sheasby for unlimited use of the Plint machine. Thanks are also given to the staff of the Synchrotron Radiation Centre (SRC), University of Wisconsin, Madison, for their technical support and the National Science Foundation (NSF) for supporting the SRC under Award No. DMR-95-31009.

References

- [1] C.H. Bovington, in: *Chemistry and Technology of Lubricants*, eds. R.M. Mortier and S.T. Orszulik (Blackie, London, 1997) ch. 12.
- [2] D. Klamman, *Lubricants and Related Products* (Verlag Chemie, Weinheim, 1984) ch. 9.
- [3] J.S. Sheasby, T.A. Cauglin, A.G. Blahey and K.F. Laycock, *Trib. Int.* 23 (1990) 301.
- [4] F.G. Rounds, *ASLE Trans.* 18 (1975) 79.
- [5] R.J. Bird and G.D. Galvin, *Wear* 37 (1976) 143.
- [6] H. Spedding and R.C. Watkins, *Trib. Int.* 15 (1982) 9.
- [7] S. Jahanmir, *J. Tribology* 109 (1987) 577.
- [8] P.A. Willermet, J.M. Pierprzak, D.P. Dailey, R.O. Carter III, N. Lindsay, L.P. Haack and J.E. deVries, *ASME Trans.* 113 (1991) 38.
- [9] P.A. Willermet, R.O. Carter III and E.N. Boulos, *Trib. Int.* 25 (1992) 371.
- [10] P.A. Willermet, D.P. Dailey, R.O. Carter III, P.J. Schmitz, W. Zhu, J.C. Bell and D. Park, *Trib. Int.* 28 (1995) 163.
- [11] J.C. Bell, K.M. Delargy and A.M. Seeney, in: *Tribol. Ser.*, Vol. 21, ed. D. Dowson (Elsevier, Amsterdam, 1992) p. 387.
- [12] J.C. Bell and K.M. Delargy, in: *Proc. 6th International Congress on Tribology “Eurotrib 93”*, Budapest 1993.
- [13] Z. Yin, M. Kasrai, G.M. Bancroft, K.F. Laycock and K.H. Tan, *Trib. Int.* 26 (1993) 383.
- [14] Z. Yin, M. Kasrai, G.M. Bancroft, K. Fyfe and K.H. Tan, *Wear* 202 (1997) 172.
- [15] Z. Yin, M. Kasrai, M. Fuller, G.M. Bancroft, K. Fyfe, M.L. Colaianni and K.H. Tan, *Wear* 202 (1997) 192.
- [16] M. Fuller, Z. Yin, M. Kasrai, G.M. Bancroft, E.S. Yamaguchi, P.R. Ryason, P.A. Willermet and K.H. Tan, *Trib. Int.* 30 (1997) 305.
- [17] M.L. Suominen Fuller, M. Kasrai, G.M. Bancroft, K. Fyfe and K.H. Tan, *Trib. Int.* 31 (1999) 627.
- [18] M. Kasrai, W.N. Lennard, R.W. Brunner, G.M. Bancroft, J.A. Bardwell and K.H. Tan, *Appl. Surf. Sci.* 99 (1996) 303.
- [19] Z. Yin, *Chemistry of antiwear films by X-ray absorption spectroscopy*, Ph.D. thesis, University of Western Ontario, London, Ontario, Canada (1995).
- [20] J.M. Martin, *Trib. Lett.* 6 (1999) 1.
- [21] K. Varlot, J.M. Martin, B. Vacher and K. Inoue, in: *Proc. of the Leeds–Lyon Symposium*, September 1998.
- [22] L.L. Cao, Y.M. Sun and L.Q. Zheng, *Wear* 140 (1990) 345.
- [23] W.A. Glaeser, D. Baer and M. Engelhardt, *Wear* 162–164 (1993) 132.
- [24] C. Jansson, G.T. Nielsen, J. Jakobsen and P. Morgen, *J. Vac. Sci. Technol. A* 11 (1993) 183.
- [25] S. Contarini, G. Tripaldi, G. Ponti, S. Lizzit, A. Baraldi and G. Paolucci, *Appl. Surf. Sci.* 108 (1997) 359.
- [26] A.L. Pidduck and G.C. Smith, *Wear* 212 (1997) 254.
- [27] O.L. Warren, J.F. Graham, P.R. Norton, J.E. Houston and T.A. Michalske, *Trib. Lett.* 4 (1998) 189.
- [28] J.F. Graham, C. McCague and P.R. Norton, *Trib. Lett.* 6 (1999) 149.
- [29] H. Ade, J. Kirtz, H. Rarback, S. Hulbert, E. Johnson, D. Kern, P. Chang and Y. Vladimirovsky, in: *X-ray Microscopy*, eds. D. Sayre, M. Howells, J. Kirtz and H. Rarback (Springer, Berlin, 1988) p. 280.
- [30] H. Ade, A.P. Smith, H. Zhang, G.R. Zhuang, J. Kirz, E. Rightor and A. Hitchcock, *J. Electron. Spectrosc. Rel. Phenom.* 84 (1997) 52.
- [31] B.P. Tonner, G.R. Harp, S.F. Koranda and J. Zhang, *Rev. Sci. Instrum.* 63 (1992) 564.
- [32] G. DeStasio, M. Capozzi, G.F. Lorusso, P.A. Baudat, T.C. Droubay, P. Perfetti, G. Margaritondo and B.P. Tonner, *Rev. Sci. Instrum.* 69 (1998) 2062.
- [33] M. Kasrai, M. Fuller, M. Scaini, Z. Yin, R.W. Brunner, G.M. Bancroft, M.E. Fleet, M. Fyfe and K.H. Tan, in: *Tribol. Ser.*, Vol. 30, ed. D. Dowson (Elsevier, Amsterdam, 1995) p. 659.
- [34] G.M. Bancroft, *Can. Chem. News* 44 (1992) 15.
- [35] M. Kasrai, Z. Yin, G.M. Bancroft and K.H. Tan, *J. Vac. Sci. Technol. A* 11 (1993) 2694.
- [36] F.G. Rounds, *ASLE Trans.* 30 (1987) 479.
- [37] E.S. Yamaguchi, P.R. Ryason, E.Q. Labrador and T.P. Hansen, *Trib. Trans.* 39 (1996) 220.
- [38] D.G. Placek and S.G. Shankwalkar, *Wear* 173 (1994) 207.
- [39] G.M. Bancroft, M. Kasrai, M. Fuller, Z. Yin, K. Fyfe and K.H. Tan, *Trib. Lett.* 3 (1997) 47.
- [40] M.L. Suominen Fuller, L. Rodriguez Fernandez, G.R. Massoumi, W.N. Lennard, M. Kasrai and G.M. Bancroft, *Trib. Lett.*, submitted.